Dilepton plus $\not{E}_T$ Signature from Two-component Dark Matter at the LHC

Shu Chen[1]
School of Physics and Astronomy, University of Southampton, UK

April 2026

[1]shu.chen@soton.ac.uk

Outline

Introduction

Why multiple-component dark matter (DM)?

- The standard model (SM) fails to explain DM.
- Traditional WIMP DM models focus on a single component.
- But the nature may have a richer dark sector beyond the SM.

Our Model

- A 3-Higgs-Doublet Model containing [1, 2]:
  - 1 active doublet $\rightarrow$ SM-like Higgs.
  - 2 inert scalar doublets $\rightarrow$ two stable scalar DM candidates.
- Stabilised by a $Z_2 \times Z_2'$ discrete symmetry.

LHC Search

- $2\ell + \not{E}_T$ signature from the production and decay from next-to-lightest particles (NLPs) in the dark sector.
- The signal will depend on the mass of the DM and mass gaps between DM and its NLPs.

$Z_2 \times Z_2'$ inert (2+1) Higgs doublet model

the Higgs doublet terms are:

$$\phi_1 = \begin{pmatrix} H_1^+ \\ \frac{H_1+iA_1}{\sqrt{2}} \end{pmatrix}, \qquad \phi_2 = \begin{pmatrix} H_2^+ \\ \frac{H_2+iA_2}{\sqrt{2}} \end{pmatrix}, \qquad \phi_3 = \begin{pmatrix} G^+ \\ \frac{v+h+iG^0}{\sqrt{2}} \end{pmatrix},$$

and the $Z_2 \times Z_2'$ discrete symmetry in our model:

$$g_{Z_2} = \mathrm{diag}(-1, 1, 1), \quad g_{Z_2'} = \mathrm{diag}(1, -1, 1),$$

In this model, the $Z_2 \times Z_2'$ symmetry makes the lightest particle in each new doublet stable, and by choosing the **neutrally charged particle** to be the lightest one, it allow us to have DM in the model.

In our work, we chose the **CP-even** components in each doublet to be the lightest particles, i.e.

$$H_1 \qquad \text{and} \qquad H_2,$$

so that it provides us a two-component DM scenario, and the decays of the heavy particles, e.g. A_1 and A_2, will lead to some experimental observations.

Model constraints

There are several constraints for our model ($n = 1, 2$).

- Avoiding the EW gauge boson decay into new scalars:

$$m_{H_n/A_n} + m_{H_n^\pm} \geq m_{W^\pm}, \quad m_{H_n} + m_{A_n} \geq m_Z, \quad 2m_{H_n^\pm} \geq m_Z.$$

- Survived mass region from LEP2 Supersymmetry particle search re-interpreted for the I(1+1)HDM [3]:

$$m_{A_n} > 100 \text{ GeV}, \quad \text{or} \quad m_{H_n} > 80 \text{ GeV}, \quad \text{or} \quad \Delta m = |m_{A_n} - m_{H_n}| < 8 \text{ GeV}.$$

- We take a lower bound on charged states from [4]:

$$m_{H_n^\pm} > 70 \text{ GeV}.$$

- DM relic density constraints [5]:

$$\Omega_{H_1} h^2 + \Omega_{H_2} h^2 = \Omega_{DM} h^2 = 0.1200 \pm 0.0012.$$

Then the model should also satisfy the theoretical constraints on aspects of perturbative unitarity, EW precision observables, the stability of the potential and the global minimum conditions [2].

Process and couplings

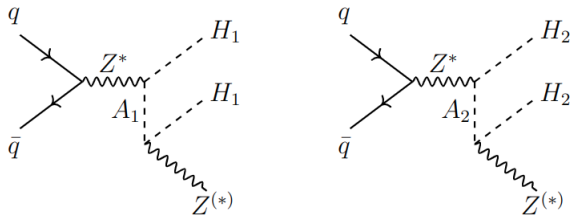

Figure: Diagrams leading to the $2\ell + \not{E}_T$ final state mediated by the Z boson.

- Small mass gap between DM and its NLPs.
- The off-shell Z boson and DM can provide us a $2\ell + \not{E}_T$ signature.

And due to the vertices in our diagrams are all in EW gauge with coupling:

$$g_{H_n A_n Z} = 1/2(g \cos\theta_W + g' \sin\theta_W).$$

The signals from this process will only be affected by the masses of DM and mass gaps between H_n and A_n from the new parameter space.

Mass scan on cross-sections

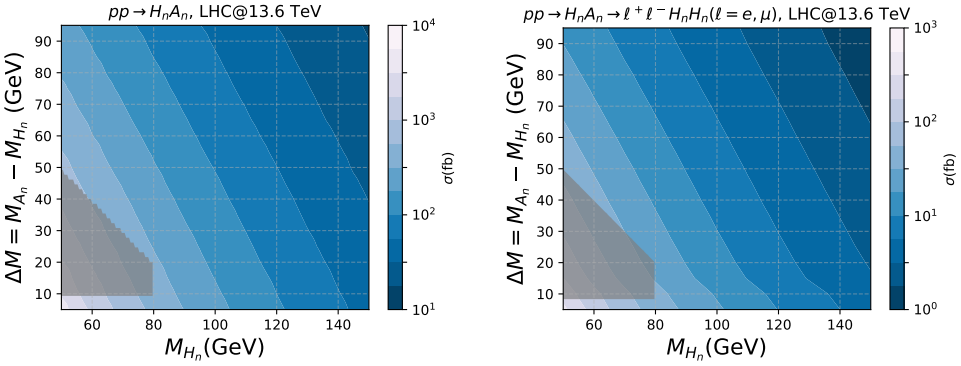

Figure: Parameter scan over masses of the DM and the mass differences between DM and NLP in each dark sector for cross-sections for the processes $pp \to H_n A_n$ and $pp \to H_n A_n \to H_n H_n \ell\ell$, and the shaded grey area was ruled out by the LEP2 re-interpretation.

Mass scan on cross-sections

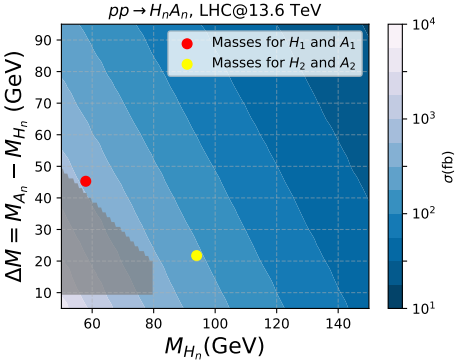

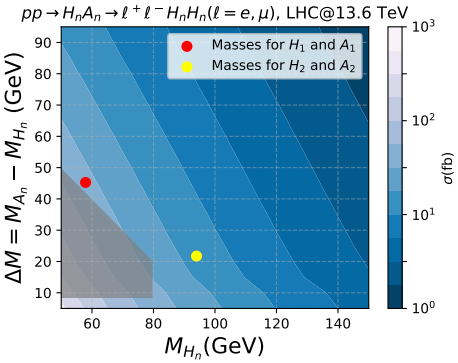

- We chose a benchmark point (BP) with masses: $m_{H_1} = 57.92$ GeV, $m_{H_2} = 93.98$ GeV, $m_{A_1} = 103.19$ GeV, and $m_{A_2} = 115.7$ GeV.
- This BP allows us to have a sufficiently large cross-section of these processes.

Detector-level distributions and background

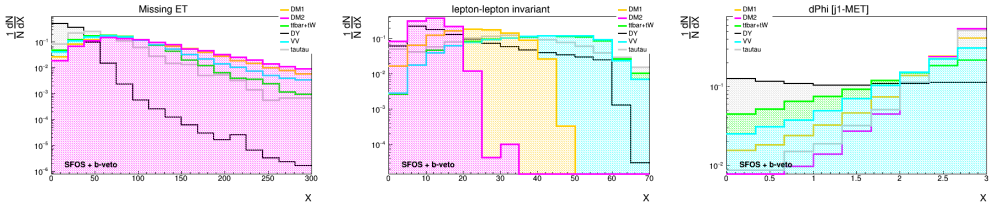

Figure: Detector-level distributions on missing transverse energy, dilepton invariant masses and separations between jet and $\not{E}_T$ for both signals and background events.[2]

- We require an initial-state radiation (ISR) jet at final state to increase $\not{E}_T$.
- detector-level Backgrounds: Drell-Yan process, $\tau\tau$, dileptonic $t\bar{t}$, tW and VV.

[2] Produced by `MadGraph5_aMC@NLO` [6] and `CheckMATE2` [7, 8, 9] which incorporates `pythia` [10] and `delphes` [11].

Fake and non-prompt lepton background

Additionally, there is a significant contribution on reducible background coming from fake and non-prompt (FNP) leptons [12].

- **Fake leptons**: lepton signals where the reconstructed object is not due to leptons, e.g. jets misidentified as leptons.
- **Non-prompt leptons**: leptons from the semileptonic decay of hadrons, e.g. b, c-mesons, or from photon conversions in detector material.

As the measurement of electron and muon signals are coming from the detector layers with different structures, which makes **fake muon** signals **negligible** and leads FNP muon signals mainly coming from **b, c-meson semileptonic decay** [12], i.e. non-prompt muons.

Therefore, in this work, we focus on the **dimuon signature**, i.e. $\ell = \mu$, to avoid the fake lepton background, and aim to construct the non-prompt muon background events in our analysis.

FNP Muons and ATLAS Opendata

We identify the most populated FNP muon source will come from the events with 1 **prompt muon** and 1 **non-prompt muon**. Therefore, we target two types of FNP muon background in our research:

$$W + \text{jets} \quad \text{and} \quad \text{Semi-muonic } t\bar{t},$$

- For $W + \text{jets}$, the $W + c$ and $W + b\bar{b}$ provide most of the FNP muons, and the jets provide FNP muon from semileptonic decay of C-hadrons and B-hadrons.
- For the Semi-muonic $t\bar{t}$, one of the b quarks provides the FNP muon from hadron's semileptonic decay.

Due to the very large cross-section of $W + \text{jets}$ (around $20nb$), we used sample #501709 in Open LHC Monte Carlo Event Generation[3] to be our events, as it provides a strong soft-muon filter filtering 99.4% of the events.

We generate semi-muonic $t\bar{t}$ in `MadGraph5_aMC@NLO`[6] with `pythia` [10]

[3] `https://opendata.atlas.cern/docs/data/for_research/evgen_data`, and a white paper will be published in arXiv soon.

Cutflows

Cuts	DM1	DM2	Drell-Yan($\mu^+\mu^-$)	dimuonic $t\bar{t}$	$Z^*/\gamma^*(\to\tau^+\tau^-)$	tW	VV(all)
All	1807.79 ± 18.08	788.81 ± 7.89	8725164.07 ± 2374.69	1635000.00 ± 3983.63	973467.60 ± 615.67	160234.93 ± 402.82	93396.10 ± 223.44
2 OS muons	391.21 ± 8.41	129.44 ± 3.20	3113354.82 ± 1418.52	827214.00 ± 1467.77	216543.00 ± 290.38	19607.30 ± 140.91	11981.51 ± 78.82
b-veto	335.89 ± 7.79	112.64 ± 2.98	2657890.00 ± 1310.65	99080.00 ± 806.21	187339.60 ± 270.09	3610.18 ± 60.41	9831.79 ± 72.06
$E_T^{miss} > 110\text{GeV}$	132.51 ± 4.89	50.25 ± 1.99	1836.13 ± 34.45	20514.00 ± 362.32	15795.84 ± 78.43	655.31 ± 25.73	2175.25 ± 34.18
$\Delta R_{ll} < 1.5$	105.94 ± 4.38	45.36 ± 1.89	1774.73 ± 33.87	4456.00 ± 168.43	11800.36 ± 67.79	419.11 ± 20.59	1363.23 ± 27.12
$P_T^{j_1} > 120\text{GeV}$	54.05 ± 3.13	29.58 ± 1.53	830.48 ± 23.17	2015.00 ± 113.22	9210.56 ± 59.89	157.42 ± 12.58	816.54 ± 21.47
$\Delta\Phi[j_1 - E_T^{miss}] > 2.0$	51.52 ± 3.05	28.71 ± 1.50	357.39 ± 15.20	1837.00 ± 108.10	9069.99 ± 59.43	146.02 ± 12.13	767.83 ± 20.90
$\Delta\Phi[Jets - E_T^{miss}] > 0.4$	47.91 ± 2.94	25.56 ± 1.42	142.18 ± 9.59	1186.00 ± 32.85	8515.89 ± 57.58	119.41 ± 10.95	696.26 ± 19.90
$m_{\tau\tau}$ cut	37.42 ± 2.60	22.64 ± 1.34	126.03 ± 9.02	991.00 ± 79.41	1186.47 ± 21.49	100.47 ± 10.05	579.32 ± 18.11
$M_{T2}(\text{tau}) > 20\text{GeV}$	32.18 ± 2.41	15.70 ± 1.11	107.28 ± 8.33	794.00 ± 71.08	61.52 ± 4.89	85.39 ± 9.27	512.08 ± 16.96
$M_{T2}(\text{top}) > 180\text{GeV}$	22.96 ± 2.04	10.25 ± 0.90	57.52 ± 6.10	242.00 ± 14.87	36.99 ± 3.80	38.98 ± 6.26	378.47 ± 14.74
$m_{ll} < 50$ GeV	22.96 ± 2.04	10.25 ± 0.90	56.23 ± 6.03	131.00 ± 10.92	28.81 ± 3.35	31.71 ± 5.64	309.33 ± 13.28

Table: Cutflow for the signal and background (with 2 prompt muons) normalized events for LHC Run-III with $\sqrt{s} = 13.6$ TeV and luminosity $300fb^{-1}$.

Total DM	Total SM	$S/\sqrt{B}$ at LHC ($300fb^{-1}$ ($3ab^{-1}$))
33	557	1.41(4.45)

Table: Signal significance for LHC Run-III with $\sqrt{s} = 13.6$ TeV and luminosity $300fb^{-1}$(HL-LHC luminosity of $3ab^{-1}$).

If we combine the ATLAS and CMS data, $S/\sqrt{B}$ will be multiplied by a factor of $\sqrt{2}$.

Distribuiton after cuts

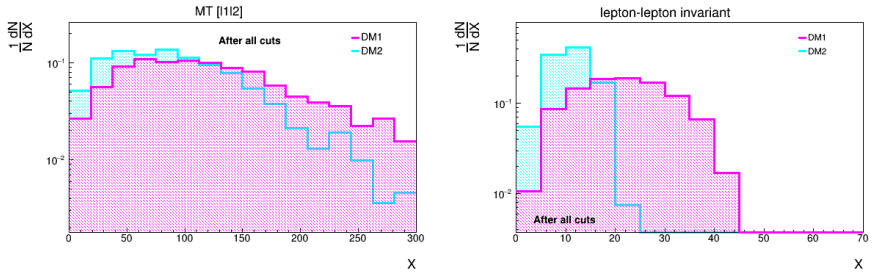

Figure: Detector-level distributions for dimuon pairs after all cuts in table 1 for H_1 and H_2.

- The signal distribution after all cuts shows two different patterns as we expected.
- It can confirm the presence of two-component DM at the LHC and also the mass spectrum of the inert particles.

Mass scan on efficiency and significance

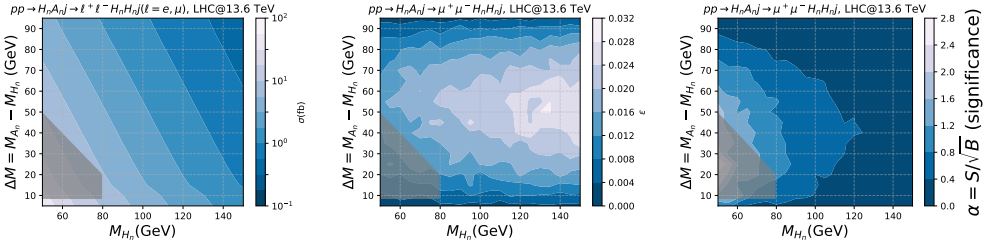

Figure: Parameter scan over masses of the DM and the mass differences between DM and NLP in each dark sector for cross-section efficiency and significance for process of $pp \to H_n A_n j \to H_n H_n \mu\mu j$, and the shaded grey area was ruled out by the LEP2 re-interpretation.

Summary

Discussion:

- Exploration a two-component scalar DM model: I(2+1)HDM with $Z_2 \times Z_2'$ symmetry.
- Simulation on a $2\ell + \not{E}_T$ signature at the LHC.
- A full detector-level analysis showing that the signal is detectable at the LHC.
- The method shows a model-independent parameterisation using DM mass and mass splitting for multi-component DM searches,
- Also suitable for interpretations in other two-component scalar DM models providing $2\ell + \not{E}_T$ signals.

Next steps:

- Finalising the non-prompt muon background estimation in our analysis.
- Developing a similar analysis for Z_2 I(2+1)HDM DM searches.

Thank you!

References I

Jaime Hernandez-Sanchez, Venus Keus, Stefano Moretti, and D Sokołowska.
Complementary collider and astrophysical probes of multi-component dark matter.
Journal of High Energy Physics, 2023(3):1–22, 2023.

J Hernandez-Sanchez, V Keus, S Moretti, D Rojas-Ciofalo, and D Sokolowska.
Complementary probes of two-component dark matter.
arXiv preprint arXiv:2012.11621, 2020.

Erik Lundström, Michael Gustafsson, and Joakim Edsjö.
Inert doublet model and lep ii limits.
Physical Review D, 79(3), February 2009.

Aaron Pierce and Jesse Thaler.
Natural dark matter from an unnatural higgs boson and new colored particles at the tev scale.
Journal of High Energy Physics, 2007(08):026–026, August 2007.

References II

N. Aghanim et al.
Planck2018 results: Vi. cosmological parameters.
Astronomy amp; Astrophysics, 641:A6, September 2020.

J. Alwall, R. Frederix, S. Frixione, V. Hirschi, F. Maltoni, O. Mattelaer, H. S. Shao, T. Stelzer, P. Torrielli, and M. Zaro.
The automated computation of tree-level and next-to-leading order differential cross sections, and their matching to parton shower simulations.
JHEP, 07:079, 2014.

Manuel Drees, Herbi Dreiner, Daniel Schmeier, Jamie Tattersall, and Jong Soo Kim.
CheckMATE: Confronting your Favourite New Physics Model with LHC Data.
Comput. Phys. Commun., 187:227–265, 2015.

References III


Jong Soo Kim, Daniel Schmeier, Jamie Tattersall, and Krzysztof Rolbiecki.
A framework to create customised LHC analyses within CheckMATE.
Comput. Phys. Commun., 196:535–562, 2015.


Daniel Dercks, Nishita Desai, Jong Soo Kim, Krzysztof Rolbiecki, Jamie Tattersall, and Torsten Weber.
CheckMATE 2: From the model to the limit.
Comput. Phys. Commun., 221:383–418, 2017.


Christian Bierlich et al.
A comprehensive guide to the physics and usage of PYTHIA 8.3.
SciPost Phys. Codeb., 2022:8, 2022.

References IV


J. de Favereau, C. Delaere, P. Demin, A. Giammanco, V. Lemaître, A. Mertens, and M. Selvaggi.
DELPHES 3, A modular framework for fast simulation of a generic collider experiment.
JHEP, 02:057, 2014.


Georges Aad et al.
Tools for estimating fake/non-prompt lepton backgrounds with the ATLAS detector at the LHC.
JINST, 18(11):T11004, 2023.


Zhenyu Han, Graham D. Kribs, Adam Martin, and Arjun Menon.
Hunting quasidegenerate Higgsinos.
Phys. Rev. D, 89(7):075007, 2014.

References V

Howard Baer, Azar Mustafayev, and Xerxes Tata.
Monojet plus soft dilepton signal from light higgsino pair production at LHC14.
Phys. Rev. D, 90(11):115007, 2014.

Alan Barr and James Scoville.
A boost for the EW SUSY hunt: monojet-like search for compressed sleptons at LHC14 with 100 fb^1.
JHEP, 04:147, 2015.

Appendix - Parton-level distributions

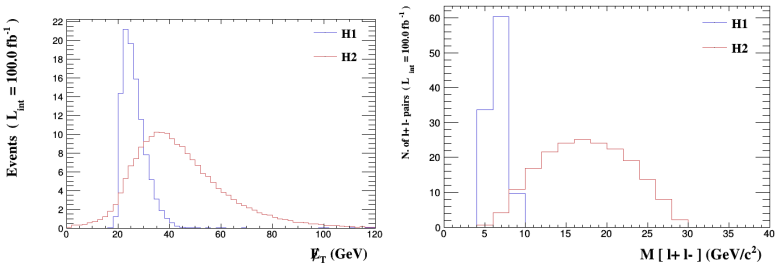

Figure: Parton level distributions on missing transverse energy and invariant mass of dilepton pairs for $Z_2 \times Z_2'$ i3HDM in [1]

We can clearly see there will be two different patterns for this two-component DM model. It not only allows us to prove the existence of two DM states at the same time, but also confirms the mass spectrum of the inert particles.

Appendix - Selections

1. Exactly two tight opposite-sign muons ($\mu^+\mu^-$).
2. A veto on b-jet to suppress backgrounds from $t\bar{t}$ and tW productions.
3. Missing transverse energy $\not{E}_T$. must be greater than 110 GeV
4. ΔR between the two SFOS muons must obey $\Delta R(l^+l^-) < 1.5$.
5. The transverse momentum of the leading jet must obey $p_T^{j_1} > 120$ GeV.
6. $\Delta\phi$ between the leading jet and $\not{E}_T$ must be above 2.0 to eradicate the DY background where $\not{E}_T$ comes solely from the presence of the jet.
7. $\Delta\phi$ between any jet and $\not{E}_T$ must be above 0.4.
8. Reconstruct $m_{\tau\tau}$ by assuming energetic tau production in the $Z^{(*)}/\gamma^{(*)}(\rightarrow \tau\tau) + j$ process, i.e. considering ν's are highly collinear with the μ's, and cut out the range for $0 < m_{\tau\tau} < 160$GeV[13, 14, 15].
9. $M_{T2}(\ell_1, \ell_2, E_T^{miss}) = \min_{\vec{q}_T^{(1)} + \vec{q}_T^{(1)} = \vec{p}_T^{miss}}[\max(M_T(\vec{p}_T^{\ell_1}, \vec{q}_T^{(1)}), M_T(\vec{p}_T^{\ell_2}, \vec{q}_T^{(2)}))] < 20$GeV
10. $M_{T2}(\text{top}) = \min[M_{T2}(\ell_1 + \text{jet}_1, \ell_2 + \text{jet}_2, E_T^{miss}), M_{T2}(\ell_1 \leftrightarrow \ell_2)] > 180$GeV
11. The invariant mass must satisfy $m_{ll} < 50$ GeV in order to avoid contributions from on-shell Z-boson decays.

Appendix - Potential

The Higgs potential for $Z_2 \times Z_2'$ i3HDM is

$$
\begin{aligned}
V &= V_0 + V_{Z_2\times Z_2'}, \\
V_0 &= -\mu_1^2(\phi_1^\dagger\phi_1) - \mu_2^2(\phi_2^\dagger\phi_2) - \mu_3^2(\phi_3^\dagger\phi_3) + \lambda_{11}(\phi_1^\dagger\phi_1)^2 + \lambda_{22}(\phi_2^\dagger\phi_2)^2 + \lambda_{33}(\phi_3^\dagger\phi_3)^2 \\
&\quad +\lambda_{12}(\phi_1^\dagger\phi_1)(\phi_2^\dagger\phi_2) + \lambda_{23}(\phi_2^\dagger\phi_2)(\phi_3^\dagger\phi_3) + \lambda_{31}(\phi_3^\dagger\phi_3)(\phi_1^\dagger\phi_1) \\
&\quad +\lambda_{12}'(\phi_1^\dagger\phi_2)(\phi_2^\dagger\phi_1) + \lambda_{23}'(\phi_2^\dagger\phi_3)(\phi_3^\dagger\phi_2) + \lambda_{31}'(\phi_3^\dagger\phi_1)(\phi_1^\dagger\phi_3), \\
V_{Z_2\times Z_2'} &= \lambda_1(\phi_1^\dagger\phi_2)^2 + \lambda_2(\phi_2^\dagger\phi_3)^2 + \lambda_3(\phi_3^\dagger\phi_1)^2 + \text{h.c.},
\end{aligned}
$$